Sensitivity Limits and Functional Characteristics of Fluxgate Sensors with Rod-Shaped Magnetic Cores

Dominika Kopala, Anna Ostaszewska-Liżewska
Warsaw University of Technology, Institute of Metrology and Biomedical Engineering, sw. A. Boboli 8; PL-02-525 Warsaw, Poland

Roman Szewczyk
Łukasiewicz Research Network – Industrial Research Institute for Automation and Measurements PIAP, Al. Jerozolimskie 202, PL-02-486, Warsaw, Poland

Abstract: Highly sensitive fluxgate magnetic field sensors with rod-shaped cores are widely used for non-destructive testing as well as for industrial applications. However, in case of both Foerster and Vacquier (two-core sensors configurations), fluxgate sensors sensitivity is directly connected with the relative magnetic permeability of the sensor's core. It should be highlighted that the magnetic permeability of rod-shaped magnetic cores is driven mainly by the demagnetization factor determined by its slenderness (aspect ratio). The paper presents the analyses of sensitivity limits of fluxgate sensors with rod-shaped cores. On the base of estimations of demagnetization factor specific for fluxgate sensors, it is shown that in case of rod-shaped cores, the sensor's sensitivity is connected with the shape of the core rather than its relative magnetic permeability. This conclusion is essential during the development and optimization of functional characteristics of fluxgate sensors.

Keywords: fluxgate sensors, demagnetization coefficient, magnetic permeability

1. Wprowadzenie

High-resolution magnetic field measurements play a significant role in many different technological and scientific research areas such as nondestructive testing [1, 5], dangerous objects detection [12] and demining [6], archeological [18] and geological studies [19] as well as space research [21]. In spite of radical advancements in the development of magnetoresistive [8] and magnetoimpedance sensors [4], fluxgate sensors [14] are the most crucial sensor type for room temperature, high resolution, and nearly constant magnetic field measurements.

Commonly used fluxgate sensors appear in three main configurations: Foerster configuration [3], Vacquier configuration [15] and ring-shaped core configurations [13]. Highly sensitive fluxgate sensors in Foerster and Vacquier configurations, highly sensitive fluxgate sensors utilize rod-shaped cores made of high permeability soft magnetic materials like permalloy [7] or supermalloy [20]. However, due to the open magnetic circuit of the rod-shaped core, it is observed that magnetic permeability is significantly reduced by demagnetization factor N [10].

Autor korespondujący:
Roman Szewczyk, roman.szewczyk@piap.lukasiewicz.gov.pl

Artykuł recenzowany
nadesłany 30.05.2022 r., przyjęty do druku 20.06.2022 r.

Despite the fact that those general calculations of demagnetization factor N for rod-shaped cores were widely presented in the literature [17, 8], the demagnetization factor is considered as the averaged result for the whole rod-shaped core's length. On the other hand, in the case of fluxgate sensor in Foerster or Vacquier configuration, only a part of its core influences the sensor's sensitivity. As a result, assessing the effect of demagnetization on the fluxgate sensor's functional characteristic should be carried out on specific data considering the particular sensor's construction.

Present paper is filling the gap in the state of art by presenting the finite element method (FEM) based solution for estimation of the influence of the demagnetization process on the sensitivity of fluxgate sensor. Presented results indicate that understanding of the demagnetization factor plays a key role in efficient material selection and construction of fluxgate sensors in both Foerster and Vacquier configuration.

2. Principles of operation of the fluxgate sensor

Geometric model of fluxgate sensors in Vacquier and Foerster configurations are presented in figures 1a and 1b, respectively. In both configurations fluxgate sensor consists of two rod-shaped cores (1), two cylindrical magnetizing windings (2), and one or two sensing windings (3), depending on the sensor's configuration. It should be highlighted that in case of fluxgate sensors with rod-shaped cores, due to the configuration of elec-

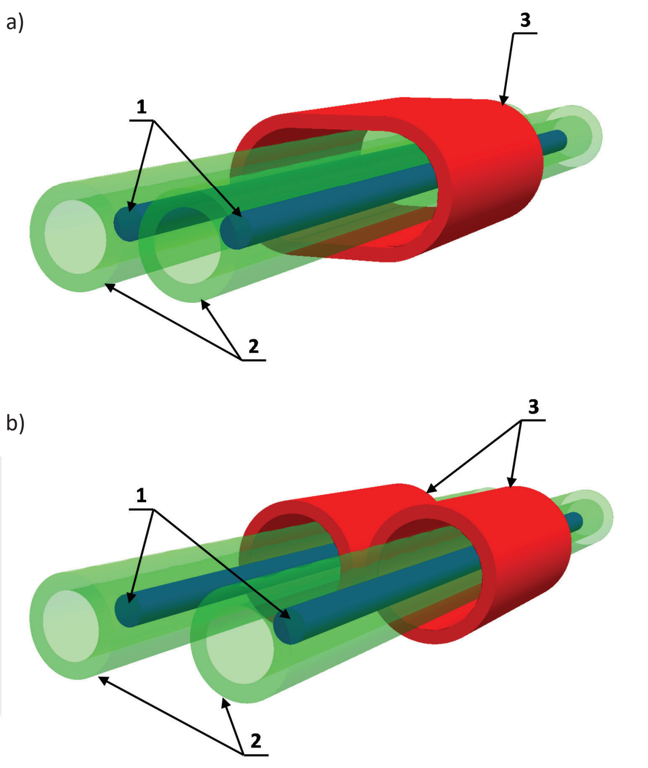

Fig. 1. Geometric models of fluxgate sensors in: a) Vacquier, b) Foerster configurations. 1 – two rod-shaped cores, 2 – two cylindrical magnetizing windings, 3 – one or two sensing windings (3)
Rys. 1. Geometria modeli czujników fluxgate w konfiguracjach: a) Vacquier'a, b) Foerster'a. 1 – dwa rdzenie prętowe, 2 – dwa cylindryczne uzwojenia magnesujące, 3 – jedno lub dwa uzwojenia pomiarowe (3)

trical connection of the windings, magnetizing cylindrical coils generate magnetizing field in the opposite directions.

In case of sinewave driving current with the amplitude I_A, magnetizing fields H_1 and H_2 in the sensor's core can be calculated as:

$$H_1 = H_m + k_m I_A \sin(2\pi f t) \quad (1)$$

$$H_2 = H_m - k_m I_A \sin(2\pi f t) \quad (2)$$

where H_m is measured, the external magnetic field, f is the driving current frequency, t is time, and k_m is the cylindrical driving coil shape factor connecting the current driving with generated magnetizing field.

Magnetic flux density B in the core can be calculated as:

$$B_1 = \mu_0 \mu_{rc} H_1 \quad (3)$$

$$B_2 = \mu_0 \mu_{rc} H_2 \quad (4)$$

where m_0 is the magnetic constant and m_{rc} is the relative magnetic permeability of a rod-shaped core at the length covered by the sensing winding (3) presented in figure 1. In recently developed fluxgate sensors, sensing winding covers typically 1/3 of the rod-shaped core's length. Moreover, due to the non-uniform magnetization of the rod-shaped core [9], the relative magnetic permeability m_{rc} of the core should be averaged at length covered by sensing winding. It should be highlighted that relative magnetic permeability of the rod-shaped core m_{rc} is limited by the relative magnetic permeability m_r of the core's material. It is significantly smaller and dependent on the length/diameter relation of the shape of the core.

Finally, the output voltage signal U at the sensing winding can be calculated as:

$$U = k_V \frac{d(B_1 + B_2)}{dt} \quad (5)$$

for Vacquier configuration and:

$$U = k_F \left[\frac{d(B_1)}{dt} + \frac{d(B_2)}{dt} \right] \quad (6)$$

for Foerster configuration. In equations (5) and (6) k_V and k_F are the factors describing the cross-section of rod-shaped cores and the number of turns of sensing coil windings in Vacquier and Foerster sensor configuration, respectively.

In both Vacquier and Foerster fluxgate sensor configurations, the core has to be deeply saturated during each magnetization cycle [14]. In such a case, the second harmonic of a driving signal should be considered as the output signal at the sensing coil [14]. It can be proved that for the linear approximation of $B(H)$ core characteristic with core magnetic relative permeability m_{rc} and saturation at flux density B_s, the amplitude of the second harmonic at the sensing coil is proportional to the core's relative permeability m_{rc}. However, it should be highlighted that m_{rc} is the relative magnetic permeability of the part of a rod-shaped core covered by the sensing coil, not the relative magnetic permeability m_r connected to the properties of the core's material.

3. Finite element method (FEM) based modeling

Previously presented methods of assessing the demagnetization factor N of rod-shaped cores consider the whole length of the core [9]. To consider only the magnetization of its central part at 1/3 of the core's length, the finite element method (FEM) should be used.

In the presented research, the open-source FEM toolchain consisting of NETGEN [20], Elmer FEM [23], and ParaVIEW [24] was used. First, a tetrahedral mesh was generated on the base of Delaunay triangulation [16] with NETGEN. Next, the Whitney edge element method [2] was used to solve the magnetic system with Elmer FEM and determine the magnetization distribution in the rod-shaped core. Finally, results were visualized with ParaVIEW and quantitatively analyzed with OCTAVE [25], the open-source MATLAB [26] alternative.

Modeling was carried out for the set of values of relative material permeability m_r. The linear model with saturation was

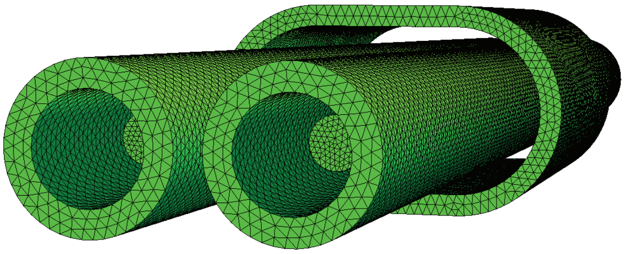

Fig. 2. The tetrahedral mesh of fluxgate sensor in Vacquier configuration. Mesh generated with open-source NETGEN software
Rys. 2. Tetrahedralna siatka czujnika fluxgate w konfiguracji Vacquier'a. Siatka wygenerowana za pomocą oprogramowania NETGEN o otwartym kodzie źródłowym

implemented for the magnetizing curve. However, for measured magnetic field H_m it was considered that its value is significantly lower than the saturation. The analysis of magnetization in the part of the sensor's core covered by sensing winding was performed for different values of L/D parameter, where L is a constant core's length equal to 100 mm, whereas D is the core's diameter.

4. Results of modeling

The results of modeling relative magnetic permeability of the part of a core covered by sensing winding are presented in figure 3. It can be observed that the core's magnetic permeability is mostly determined by the L/D factor for high permeability materials. Moreover, to achieve high magnetic permeability of the core, resulting in a high fluxgate sensor's magnetic permeability, the L/D factor should exceed 60.

On the base of the proposed method of modeling, the sensitivity S of relative core magnetic permeability to the changes

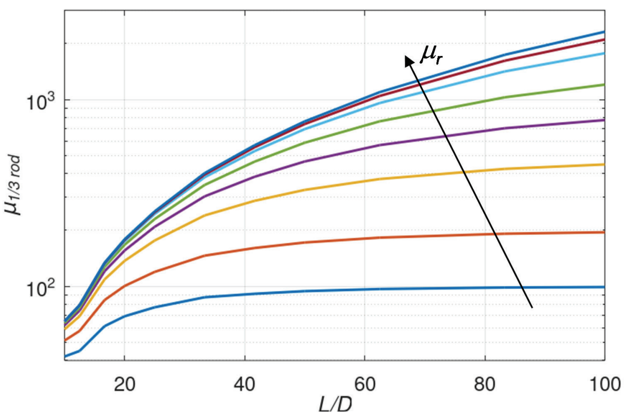

Fig. 3. The relative magnetic permeability μ of the part of a core of fluxgate sensor covered by the sensing winding as a function of core's length *L* to diameter *D* factor. Calculated for different values of relative magnetic permeability of core's material m_r = 100, 200, 500, 1 000, 2 000, 5 000, 10 000 and 20 000

Rys. 3. Względna przenikalność magnetyczna μ części rdzenia czujnika fluxgate objętej uzwojeniem detekcyjnym jako funkcja długości rdzeni *L* w zależności od średnicy *D*. Wyniki dla różnych wartości względnej przenikalności magnetycznej materiału rdzeni m_r = 100, 200, 500, 1000, 2000, 5000, 10 000 i 20 000

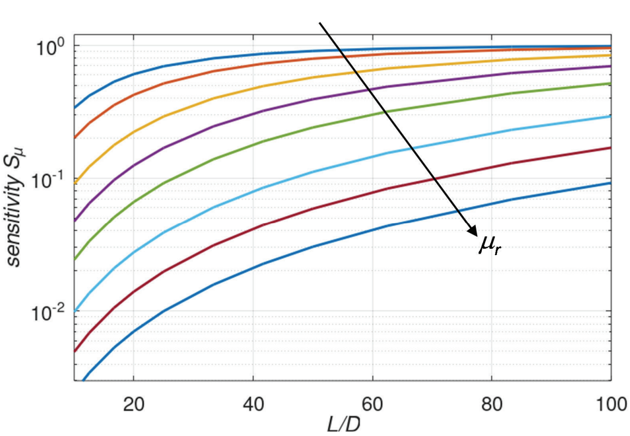

Fig. 4. The dependence of core's relative magnetic permeability sensitivity on core's length *L* to diameter *D* factor. Calculated for different values of relative magnetic permeability of core's material m_r = 100, 200, 500, 1 000, 2 000, 5 000, 10 000 and 20 000

Rys. 4. Zależność wrażliwości względnej przenikalności magnetycznej rdzenia od długości rdzenia *L* do współczynnika średnicy D. Wyniki dla różnych wartości względnej przenikalności magnetycznej materiału rdzenia m_r = 100, 200, 500, 1 000, 2 000, 5 000, 10 000 and 20 000

of relative materials magnetic permeability was calculated. This sensitivity is defined as:

$$S = \frac{\Delta\mu_{rc}}{\Delta\mu_r} \tag{7}$$

and was calculated for 10% change of material's relative magnetic permeability.

Presented results clearly indicate that the sensitivity S of core's relative magnetic permeability significantly decreases for higher values of relative magnetic permeability of core's materials. For relative magnetic permeability of core's material m_{rc} about 20 000 and L/D factor equal to 60, the reduction of material's magnetic permeability results in about 70 times less reduction of core's magnetic permeability. This phenomenon should be taken into consideration during the development, material selection as well as during the exploitation of fluxgate sensors.

5. Conclusions

Finite element method-based calculation presented in the paper enables the assessment of the influence of demagnetization process on the sensitivity of fluxgate sensors with rod-shaped cores in both Vacquier and Foerster configurations. The proposed method considers that the sensing coil of the fluxgate sensor covers only the part of the rod. As a result, previously determined demagnetization factors for the rods can't be easily adapted. It should be highlighted that the proposed method utilizes only open-source software, which significantly reduces the costs of the possible practical application of the proposed method.

The results of modeling clearly indicate that to reduce demagnetization, the core's length to diameter L/D factor should exceed 60. Moreover, for rod-shaped cores, the increase of core material relative magnetic permeability doesn't significantly influence the functional properties of fluxgate sensors. Furthermore, the increase of core's material magnetic permeability reduces the sensitivity of relative core magnetic permeability to the changes of relative material's magnetic permeability. The results of modelling indicates that for relative magnetic permeability of core's material m_{rc} about 20 000 and L/D factor equal 60 (which is a typical value for practical applications of fluxgate sensors), the reduction of material's magnetic permeability results in about 70 times less reduction of core's magnetic permeability. Such a significant reduction of core's sensitivity changes of material's relative magnetic permeability is valuable from the point of view of development, material selection and the exploitation of fluxgate sensors.

Bibliography

1. Claycomb J.R., Brazdeikis A., Le M., Yarbrough R.A., Gogoshin G., Miller J.H., *Nondestructive testing of PEM fuel cells*, "IEEE Transactions on Applied Superconductivity", Vol. 13, No. 2, 2003, 211–214, DOI: 10.1109/TASC.2003.813687.
2. Dibben D.C., Metaxas R., *A comparison of the errors obtained with Whitney and linear edge elements*, "IEEE Transactions on Magnetics", Vol. 13, No. 2, 1997, 1524–1527, DOI: 10.1109/20.582551.
3. Gaffney C., Gaffney V., Cuttler R., Yorston R., *Initial results using GPS navigation with the Foerster magnetometer system at the World Heritage site of Cyrene, Libya.*

"Archaeological Prospection", Vol. 15, No. 2, 2008, 151–156, DOI: 10.1002/arp.330.

4. Gazda P., Szewczyk R., *Novel Giant Magnetoimpedance Magnetic Field Sensor*, "Sensors", Vol. 20, No. 3, 2020, DOI: 10.3390/s20030691.
5. Wei G., Chu J., *A transducer made up of fluxgate sensors for testing wire rope defects*. "IEEE Transactions on Instrumentation and Measurement", Vol. 51, No. 1, 2002, 120–124, DOI: 10.1109/19.989914.
6. Gürkan S., Karapınar M., Doğan S., *Detection and Imaging of Underground Objects for Distinguishing Explosives by Using a Fluxgate Sensor Array*. "Applied Sciences", Vol. 9, No. 24, 2019, DOI: 10.3390/app9245415.
7. Lei J., Lei, C. Zhou Y., *Analysis and comparison of the performance of MEMS fluxgate sensors with permalloy magnetic cores of different structures*. "Measurement", Vol. 46, No. 1, 2013, 710–715, DOI: 10.1016/j.measurement.2012.09.009.
8. Joseph R.I., *Ballistic Demagnetizing Factor in Uniformly Magnetized Cylinders*. "Journal of Applied Physics", Vol. 37, No. 13, 1966, DOI: 10.1063/1.1708110.
9. Joseph R.I., Schlömann E., *Demagnetizing Field in Nonellipsoidal Bodies*. "Journal of Applied Physics", Vol. 36, No. 5, 1965, DOI: 10.1063/1.1703091.
10. Matyuk V.F., Osipov A.A., *Central demagnetization factor for bodies with different shapes. II. Rectangular rods*. "Russian Journal of Nondestructive Testing", Vol. 36, 2000, 27–32, DOI: 10.1007/bf02759390.
11. Morten B., De Cicco G., Prudenziati M., Masoero A., Mihai G., *Magnetoresistive thick film sensor for linear displacements*. "Sensors and Actuators A: Physical", Vol. 46, No. 1–3, 1995, 261–265, DOI: 10.1016/0924-4247(94)00902-t.
12. Note N., Saey T., Gheyle W., Stichelbaut B., Van den Berghe H., Bourgeois J., Van Eetvelde V., Van Meirvenne M., *Evaluation of fluxgate magnetometry and electromagnetic induction surveys for subsurface characterization of archaeological features in World War 1 battlefields*. "Geoarchaeology", Vol. 34, No. 2, 2018, 136–148, DOI: 10.1002/gea.21700.
13. Primdahl F., Brauer P., Merayo J.M.G., Nielsen O.V., *The fluxgate ring-core internal field*, "Measurement Science and Technology", Vol. 13, 2002, DOI: 10.1088/0957-0233/13/8/312.
14. Ripka P., *Review of fluxgate sensors*. "Sensors and Actuators A: Physical", Vol. 33, No. 3, 1992, 129-141, DOI: 10.1016/0924-4247(92)80159-z.
15. Ripka P., Janosek M., Butta M., Billingsley S.W., Wakefield E., *Crossfield effect in magnetic sensors*. "Sensors", 2009, DOI: 10.1109/icsens.2009.5398405.
16. Rui Y., Wang J., Qian C., Liu J., Li X., A new compound algorithm study for Delaunay triangulation construction. 2007, SPIE Proceedings, Vol. 6751, DOI: 10.1117/12.759487.
17. Sato M., Ishii Y., *Simple and approximate expressions of demagnetizing factors of uniformly magnetized rectangular rod and cylinder*. "Journal of Applied Physics", Vol. 66, No. 2, 1989, DOI: 10.1063/1.343481.
18. Smriglio F., Papale E., Verga F., Piro S., N*oninvasive geophysical integrated survey at Madonna del Giglio* (*Sabine necropolis, Magliano Sabina, Latium, Central Italy*). "Archaeological and Anthropological Sciences", Vol. 12, 2020, DOI: 10.1007/s12520-020-01029-x.
19. Topal U., Can H., Çelik O.M., Narman A., Kamiş M., Çıtak V., Çakrak D., Sözeri H., Svec P., *Design of Fluxgate Sensors for Different Applications from Geology to Medicine*. "Journal of Superconductivity and Novel Magnetism", Vol. 32, 2018, 839–844, DOI: 10.1007/s10948-018-4781-x.
20. Topal U., Svec P., Can H., Celik F., Birlikseven C., Skorvanek I., Andrejka F., Kunca B., Marcin J., Svec P., Janotova I., Uygur A., *Optimization of the Temperature Stability of Fluxgate Sensors for Space Applications*. "IEEE Sensors Journal", Vol. 21, No. 3, 2021, 2749–2756, DOI: 10.1109/jsen.2020.3024547.
21. Turner S., Hall M.J., Harmon S.A.C., Hillier N., *Calibration of a Novel Three-Axis Fluxgate Gradiometer for Space Applications*, "IEEE Transactions on Magnetics", Vol. 51, No. 1, 2015, DOI: 10.1109/tmag.2014.2360614.

Other sources

22. https://ngsolve.org/
23. https://github.com/ElmerCSC/elmerfem
24. https://www.paraview.org/
25. https://www.gnu.org/software/octave/index
26. https://www.mathworks.com/products/matlab.html

Granice czułości i charakterystyki funkcjonalne czujników fluxgate z rdzeniami magnetycznymi w kształcie prętów

Streszczenie: Bardzo czułe sensory pola magnetycznego typu fluxgate z rdzeniami w kształcie prętów są szeroko stosowane w badaniach nieniszczących, jak również w zastosowaniach przemysłowych. Jednak zarówno w przypadku czujnika w konfiguracji Foerster'a, jak i Vacquier'a (obie konfiguracje dotyczą sensorów dwurdzeniowych) ich czułość jest bezpośrednio związana ze względną przenikalnością magnetyczną rdzeni. Należy podkreślić, że o przenikalności magnetycznej prętowych rdzeni magnetycznych decyduje przede wszystkim współczynnik rozmagnesowania określony przez jego smukłość (proporcje). W artykule przedstawiono analizę granic czułości sensorów typu fluxgate z rdzeniami prętowymi. Na podstawie oszacowań współczynnika rozmagnesowania charakterystycznego dla czujników typu fluxgate wykazano, że w przypadku rdzeni prętowych czułość sensora związana jest raczej z kształtem rdzenia niż z jego względną przenikalnością magnetyczną. Wniosek ten jest szczególnie ważny podczas opracowywania i optymalizacji charakterystyk funkcjonalnych czujników fluxgate.

Słowa kluczowe: czujniki fluxgate, współczynnik demagnetyzacji, przenikalność magnetyczna

Dominika Kopala, MSc Eng.
dominika.kopala.dokt@pw.edu.pl
ORCID: 0000-0003-4936-0616

A graduate of the Faculty of Mechatronics at Warsaw University of Technology. Currently she is a PhD student at the Institute of Metrology and Biomedical Engineering. Her field of interest are focused on the usage of Finite Element Method for physical phenomena modeling. Recent research topics are concerned on magnetodynamic systems, in particular on magnetic field sensors.

Anna Ostaszewska-Liżewska, PhD Eng.
anna.lizewska@pw.edu.pl
ORCID: 0000-0002-5203-8129

Assistant professor at the Institute of Metrology and Biomedical Engineering of Warsaw University of Technology. Her current research interests include: modeling sensors using the finite element method and eyetracking in human-machine interfaces with the use of artificial intelligence.

Prof. Roman Szewczyk, PhD DSc Eng.
roman.szewczyk@piap.lukasiewicz.gov.pl
ORCID: 0000-0002-1214-1009

A longtime employee of ŁUKASIEWICZ Research Network – Industrial Research Institute for Automation and Measurements PIAP. The Chairman of 2. Workgroup on Digital Support for Industry in a Team for Industrial Transformation, the Ministry of Development (2016–2017). The Member and Deputy of the Chairman of 14. Workgroup on Sensors (including biosensors) and intelligent sersor networks in the Ministry of Economy as a part of the Operational Programme Intelligent Development (2015–2018). The Coordinator of two foresight projects performed in association with enterpeneurs, where key technologies and the direction of development for Masovian Voivodeship as well as for automation, robotics and measurement techniques industry were defined. The Coordinator of two projects as a part of Applied Research Programme (NCBiR) directed on the newest technology, realized is association with domescit enterpreneurs.